AEM
Journals.ASM.org

Xylan Utilization Regulon in *Xanthomonas citri* pv. citri Strain 306: Gene Expression and Utilization of Oligoxylosides

V. Chow,[a] D. Shantharaj,[b] Y. Guo,[a] G. Nong,[a] G. V. Minsavage,[b] J. B. Jones,[b] J. F. Preston[a]

Department of Microbiology and Cell Science, University of Florida, Gainesville, Florida, USA[a]; Department of Plant Pathology, University of Florida, Gainesville, Florida, USA[b]

***Xanthomonas citri* pv. citri strain 306 (*Xcc*306), a causative agent of citrus canker, produces endoxylanases that catalyze the depolymerization of cell wall-associated xylans. In the sequenced genomes of all plant-pathogenic xanthomonads, genes encoding xylanolytic enzymes are clustered in three adjacent operons. In *Xcc*306, these consecutive operons contain genes encoding the glycoside hydrolase family 10 (GH10) endoxylanases Xyn10A and Xyn10C, the *agu67* gene, encoding a GH67 α-glucuronidase (Agu67), the *xyn43E* gene, encoding a putative GH43 α-L-arabinofuranosidase, and the *xyn43F* gene, encoding a putative β-xylosidase. Recombinant Xyn10A and Xyn10C convert polymeric 4-*O*-methylglucuronoxylan ($MeGX_n$) to oligoxylosides methylglucuronoxylotriose ($MeGX_3$), xylotriose (X_3), and xylobiose (X_2). *Xcc*306 completely utilizes $MeGX_n$ predigested with Xyn10A or Xyn10C but shows little utilization of $MeGX_n$. *Xcc*306 with a deletion in the gene encoding α-glucuronidase (*Xcc*306 Δ*agu67*) will not utilize $MeGX_3$ for growth, demonstrating the role of Agu67 in the complete utilization of GH10-digested $MeGX_n$. Preferential growth on oligoxylosides compared to growth on polymeric $MeGX_n$ indicates that GH10 xylanases, either secreted by *Xcc*306 *in planta* or produced by the plant host, generate oligoxylosides that are processed by Xyn10 xylanases and Agu67 residing in the periplasm. Coordinate induction by oligoxylosides of *xyn10*, *agu67*, *cirA*, the *tonB* receptor, and other genes within these three operons indicates that they constitute a regulon that is responsive to the oligoxylosides generated by the action of *Xcc*306 GH10 xylanases on $MeGX_n$. The combined expression of genes in this regulon may allow scavenging of oligoxylosides derived from cell wall deconstruction, thereby contributing to the tissue colonization and/or survival of *Xcc*306 and, ultimately, to plant disease.**

Xylanolytic bacteria have been well studied with respect to the enzymes that catalyze the depolymerization of methylglucuronoxylans ($MeGX_n$) and methylglucuronoarabinoxylans ($MeGAX_n$), the predominant polysaccharides comprising hemicellulose in dicots and monocots, respectively (1, 2). As components of plant cell walls, these polysaccharides serve functions important to plant growth. Characterization of the genes and their encoded enzymes that contribute to both the depolymerization of $MeGX_n$ and $MeGAX_n$ and the utilization of the products of depolymerization have led to definitions of systems that function for both the extracellular depolymerization and the assimilation of oligosaccharides, followed by the intracellular processing of these oligosaccharides. Systems involving the depolymerization of xylans with a secreted glycoside hydrolase family 10 (GH10) endoxylanase, transporters for assimilation of oligoxylosides, and intracellular glycohydrolases, including a GH67 α-glucuronidase, are notably efficient in the utilization of $MeGX_n$ and $MeGAX_n$ (3–6).

All plant-pathogenic *Xanthomonas* spp. for which genome sequence data are available contain genes orthologous to those comprising xylan utilization gene clusters encoding GH10 endoxylanases and a single gene encoding a GH67 α-glucuronidase (7). The arrangement and content of genes within these operons differentiate these species into three groups. Members of the first group include *Xanthomonas citri* pv. citri strain 306 (*Xcc*306), *Xanthomonas campestris* pv. vesicatoria, and *Xanthomonas perforans*, in which all three endoxylanase genes (*xyn10A*, *xyn10B*, and *xyn10C*) are present, along with genes further downstream of this operon encoding an additional 10 proteins. Members of the second group include *X. campestris* pv. campestris, *Xanthomonas vesicatoria*, and *Xanthomonas gardneri*, in which two of the three endoxylanase genes are present (*xyn10A* and *xyn10C*) and in which the downstream genes encoding additional proteins are absent. A third group includes *Xanthomonas oryzae* pv. oryzae, in which a different set of two endoxylanase genes are present (*xyn10A* and *xyn10B*) and in which the beta-galactosidase and gluconolactonase genes flanking *xyn10C* in other groups are incomplete. However, the genetic organization of the α-glucuronidase operon is conserved across these species, and of all other phytopathogenic bacteria for which genome sequences are available, only these species have the combination of GH10 xylanases and GH67 α-glucuronidases. The genomic organization of the xylan utilization cluster for *Xcc*306 is shown in Fig. 1.

GH10 endoxylanases of phytopathogenic species of *Xanthomonas* have been implicated in cell wall deconstruction of plant hosts and may contribute to plant disease (8, 9). The GH10/GH67 system has been genetically defined in *X. campestris* pv. campestris and shown to allow the depolymerization and efficient utilization

Received 25 September 2014 **Accepted** 8 January 2015

Accepted manuscript posted online 16 January 2015

Citation Chow V, Shantharaj D, Guo Y, Nong G, Minsavage GV, Jones JB, Preston JF. 2015. Xylan utilization regulon in *Xanthomonas citri* pv. citri strain 306: gene expression and utilization of oligoxylosides. Appl Environ Microbiol 81:2163–2172. doi:10.1128/AEM.03091-14.

Editor: J. L. Schottel

Address correspondence to J. F. Preston, jpreston@ufl.edu.

V.C. and D.S. contributed equally to this work.

doi:10.1128/AEM.03091-14

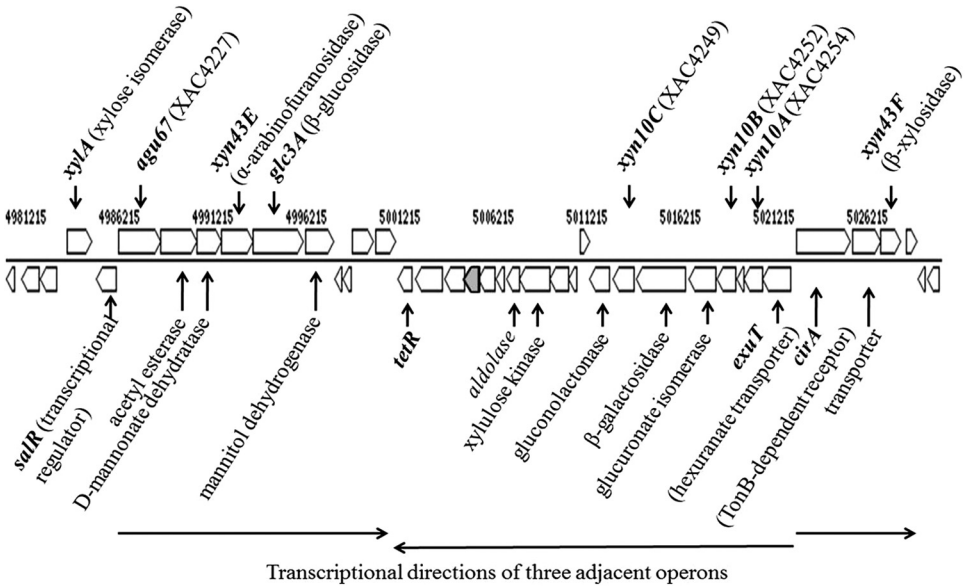

FIG 1 Cassette of operons with xylan deconstruction genes in *Xcc*306. The arrows identify sequences that are transcribed from a promoter to generate a polycistronic message.

of oligosaccharides (8). The present study is concerned with the role of endoxylanases and related enzymes collectively involved in xylan utilization for the growth of *Xcc*306 and their potential contribution to pathogenicity. *Xcc*306 shows a preferred utilization of the products of $MeGX_n$ depolymerization rather than of polymeric $MeGX_n$ and the coinduction of expression of genes encoding xylanases and neighboring genes by the products that support the growth of *Xcc*306. With the predominant localization of the xylanase activity in the periplasm, the extracellular processing of xylan appears to be a limiting step for the growth of *Xcc*306.

MATERIALS AND METHODS

Growth studies of *Xcc*306. Growth studies of *X. citri* pv. citri strain 306 (*Xcc*306) were performed by inoculating equal cell numbers grown in nutrient broth to exponential phase into the different media as specified below. The cultures were incubated at 28°C with shaking at 200 rpm. Cell growth over time was monitored by measuring optical density at 600 nm (OD_{600}), and aliquots of culture were removed when necessary for further analyses. From studies on the interaction of *X. campestris* pv. vesicatoria with its host tomato plant, two similar apoplast-mimicking media, XVM1 and XVM2 (10), which variably induce *hrp* gene expression, were constituted. $XVM2_m$ is a modified recipe of the XVM2 minimal medium and does not contain the carbohydrate carbon sources sucrose and fructose [20 mM NaCl, 10 mM $(NH_4)_2SO_4$, 1 mM $CaCl_2$, 0.01 mM $FeSO_4$, 5 mM $MgSO_4$, 0.16 mM KH_2PO_4, 0.32 mM K_2HPO_4, 0.03% Casamino Acids, pH 6.7]. Thin-layer chromatography (TLC) to detect substrate processing was performed as previously described (3).

Bacterial strains. Cultures of *Xcc*306, also known as *Xanthomonas axonopodis* pv. citri strain 306, were routinely maintained on nutrient broth agar plates as previously described (11). Construction of *Xcc*306 Δ*agu67* by mutagenesis was performed by double displacement of a portion of the *agu67* gene (XAC4227) as previously described (12). A 2,469-bp PCR product encompassing the *agu67* gene, obtained by using primers 4227F (5′-CTCTTCAAATGCGTGCAAAAGCTGC) and 4227R (5′-GTCCTGAAAAATGGGATGCAGTAGC), was cloned into the vector pGEM-T Easy. The internal BamHI fragment of 1,092 bases in the *agu67* coding sequence, which includes the bases encoding the catalytic residues D395 and E423, was deleted from the cloned gene. The partially deleted *agu67* gene was then cloned into the suicide vector pOK1 and was transformed into *Xcc*306 to eventually obtain the mutant strain *Xcc*306 Δ*agu67*. DNA sequencing of an amplicon generated by PCR confirmed the partial deletion of the *agu67* gene.

Enzyme assays. Xylanase activities with $MeGX_n$ as the substrate were determined with the Nelson reducing sugar assay to measure glycosidic bond cleavage (13). Time course assays (30 min) were performed to identify velocities representing initial velocities that could be used for estimation of kinetic parameters. The relationship between enzyme concentration and activity was determined to quantify a condition for the estimation of maximum velocity and k_{cat}. Xylanase was also assayed by the conversion of the fluorogenic substrate 6,8-difluoro-4-methylumbelliferyl β-D-xylobioside ($DiFMUX_2$) to 6,8-difluoro-4-methylumbelliferone (DiFMU) (14, 15) using an EnzChek Ultra xylanase assay kit (catalog no. E33650; Molecular Probes, Life Technologies, Grand Island, NY). One hundred-microliter reaction mixtures containing 50 μg/ml substrate and various amounts of test cell fractions in 50 mM sodium acetate, pH 6.0, were performed in 96-well plates. Reaction mixtures were incubated at room temperature for up to 2 h, and readings were taken at an excitation of 360 nm and an emission of 460 nm with a fluorescence plate reader (Synergy HT reader; Bio-Tek, Winooski, VT).

Alkaline phosphatase assays, performed according to the protocol of Bessey et al. (16), were carried out in 96-well plates with a final reaction volume of 250 μl. Ten microliters of *Xcc*306 cell fractions, obtained from exponential culture assayed for xylanase as described below, were added to 190 μl of substrate buffer containing 10 mM *p*-nitrophenylphosphate, 2.5 mM glycine, 0.05 mM $MgCl_2$, 10 mM KH_2PO_4-K_2HPO_4, adjusted to pH 10.5 with 1 N NaOH. Reaction mixtures were incubated for 30 min at 37°C and terminated by adding 50 μl of 0.085 N NaOH, and the amount of *p*-nitrophenol released was measured at 405 nm. Standard curves of *p*-nitrophenol (1 to 10 nmol) in substrate buffer were constructed to quantify *p*-nitrophenol release from the enzyme reactions. Specific activity was expressed as nmol *p*-nitrophenol released per min per OD_{600} of culture.

Determination of xylanase activities in cell fractions. Twenty-five-milliliter samples of *Xcc*306 cultures at late log phase were harvested. Cultures were subjected to centrifugation at 13,000 × *g* for 10 min at 4°C. The supernatant (culture medium), to which was added 100 μl proteinase inhibitor (Halt protease inhibitor; Thermo Scientific, Rockford, IL), was

TABLE 1 Primers used in this study

Gene locus	Gene name	Protein name (function)	Primer name (nucleotide sequence)
XAC0004	*gyrB*	GyrB (DNA gyrase subunit B)	F1472 (ACGAGTACAACCCGGACAAG)
			R1585 (GCATCTGCCGGTAGAAGAAG)
XAC3649	*atpD*	ATP-D (ATP synthase, beta subunit)	F464 (CCGTCAACATGATGGAACTG)
			R600 (CTTGTCCAGGACGTTGGAGT)
XAC4225	*xylA*	XylA (xylose isomerase)	F367 (TACGAGAGCAACCTCAAGCA)
			R490 (TCGAGGCACCATTCATGTAG)
XAC4226	*salR*	SalR (*sal* operon transcriptional repressor)	F546 (AGCCAAAGAGATCACCGAAC)
			R730 (GGCCGGATTTGTAGGTGTAA)
XAC4227	*agu67*	Agu67 (α-glucuronidase GH67)	F444 (CAGCGATATCGGGGTGTTAT)
			R600 (ATAGCCACGTTCCACCAGAC)
XAC4230	*xyn43E*	Xyn43E (arabinofuranosidase GH43)	F1050 (ACAGCCGATTCCTTACATCG)
			R1154 (GTGTGATCGAAATCGTCGTG)
XAC4237	*tetR*	TetR (transcriptional regulator)	F89 (CGACCGAGACCTACGAACAT)
			R244 (CGGACAACAGCGCATATTTA)
XAC4249	*xyn10C*	Xyn10C (endoxylanase GH10)	F328 (ACACCGGAGTGGTTCTTCAC)
			R494 (GAACGGTAACTGCCGTCTTC)
XAC4252	*xyn10B*	Xyn10B (endoxylanase GH10)	F40 (GAAACTCCGTTATCCGCTCA)
			R158 (CTTGCCGTGGGCTGTAGG)
XAC4254	*xyn10A*	Xyn10A (endoxylanase GH10)	F134 (TTGCGCAGTACTGGAACAAG)
			R284 (ACCATGACATGCATCTGGAA)
XAC4255	*exuT*	ExuT (exuronate transporter)	F794 (CCGCAGAACTGGCGTATATC)
			R946 (GCAGCCAGAACAGGAAGAAC)
XAC4256	*cirA*	TBDR (*tonB*-dependent receptor)	F122 (ACCGACGTAGCATCCAGTTC)
			R222 (ATTCATGTCCGGAAACTTGC)
XAC4258	*xyn43F*	Xyn43F (β-xylosidase GH43)	F803 (CCTACGGCCCGTTTACCTAT)
			R921 (GAGCACGCTGTCGTGATAGA)

concentrated to 2 ml or less by filtration through regenerated cellulose membranes with a 3-kDa cutoff (Amicon Ultra filters; Millipore, Billerica, MA). The cell pellets were washed twice with 10 ml 50 mM sodium acetate, pH 6.5, and resuspended in 2 ml of the acetate buffer. The resuspended cells were disrupted by two passages through a French pressure cell at 16,000 lb/in^2. Cell membranes were pelleted at 13,000 × *g* for 40 min at 4°C, and supernatants, designated cell fractions, were tested for xylanase activity.

Determination of xylanase activities in subcellular fractions. Five-milliliter cultures of *Xcc*306 were grown to late log phase in XVM2$_m$ with additional carbohydrates as specified in the figure legends. Cell fractionation was performed according to the method of Hu et al. (17). Cultures were subjected to centrifugation at 5,000 × *g* for 10 min and cells harvested. The supernatants were collected as the extracellular fractions. The cell pellets were rinsed with 10 mM $MgCl_2$ and resuspended in 30 mM Tris-HCl, pH 8.0, 1.0 mM EDTA, 20% (vol/vol) sucrose, 200 μg/ml lysozyme and incubated for 2 h on ice to lyse the outer membrane. These cell mixtures were subjected to centrifugation at 21,000 × *g* for 10 min to obtain the periplasmic fractions in the supernatants and the spheroplasts in the pellets. The pellets were resuspended in 0.25 ml 10 mM Tris-HCl, pH 8.0, passed 50 times through a syringe fitted to a 23-gauge needle, and centrifuged at 21,000 × *g* for 15 min, and the supernatants were collected as the cytoplasmic fractions. All fractions were passed through a 10-kDa cutoff filter (Micron Ultracel YM-10; Millipore) to remove residual cell debris. Fractions were concentrated to equal volumes for xylanase assays.

RNA isolation. Bacteria grown in nutrient broth (NB) to an OD_{600} of 0.3 with shaking at 200 rpm were inoculated into different media at a 1:15 ratio to a starting OD_{600} of 0.02. The bacterial cultures were incubated with shaking at 200 rpm to exponential phase, and 10 ml of each culture was collected. The bacterial samples were treated with RNAprotect reagent (Qiagen, Germantown, MD) prior to RNA extraction. Cultures were subjected to centrifugation, and cell pellets were treated with lysozyme (200 μl, 15 mg/ml) and proteinase K (10 μl, 20 mg/ml) for 10 min. RNA extractions were performed using the RNeasy minikit (Qiagen). Genomic DNA was removed from RNA samples by treatment with a Turbo DNA-free kit (Ambion, Life Technologies).

qRT-PCR. Genes from the xylan utilization cassette were chosen for expression studies with the *gyrB* and *atpD* genes, which were also tested to serve as control genes for expression outside the cassette. The primers detailed in Table 1 were designed using Primer3 software (18) and the nucleotide sequence of the *Xcc*306 genome. A one-step quantitative reverse transcription-PCR (qRT-PCR) was performed with a Bio-Rad CFX96 system (Bio-Rad, Hercules, CA) using an iScript one-step RT-PCR kit with SYBR green (Bio-Rad). The total volume of the one-step qRT-PCR mixture was 20 μl and contained 2× SYBR green RT-PCR mix (10 μl), 10 μM gene-specific primers (0.6 μl), iScript reverse transcriptase (0.4 μl), and 200 ng of the RNA template. The reaction mixtures were incubated at 50°C for 10 min and at 95°C for 5 min and then subjected to 40 cycles of 95°C for 10 s and 60°C for 30 s. Melting curve analyses were performed to verify the specificity and identities of the PCR products. Duplicate reactions were performed in each study.

Real-time quantitative-PCR data were analyzed by using the absolute quantification method as described in the real-time PCR application guide of Bio-Rad Laboratories, Inc. (19). Briefly, a known amount of *Xcc*306 genomic DNA was amplified by PCR using primers designed to amplify a segment of 200 to 250 bp of the genes of interest. Tenfold dilutions ranging from 10^2 to 10^7 genomic molecules were added as the template to the reaction mixtures, and the threshold cycle (C_T) values of the detection of products were plotted against the logarithmic values of the initial number of copies of template added. Amplification efficiency (E) was calculated from the slope of the curve using the formulae $E = 10^{-1/\text{slope}}$ and % $E = (E - 1) \times 100\%$. Several sets of primer pairs for each gene under study were designed and evaluated until 90 to 105% efficiency was achieved. A standard curve of 90 to 100% efficiency was thus generated for each optimal primer pair for each gene. The equation of linear regression, $y = mx + b$, where y is the C_T value, m is the slope of the graph, x is the logarithmic value of the number of molecules of RNA, and b is the

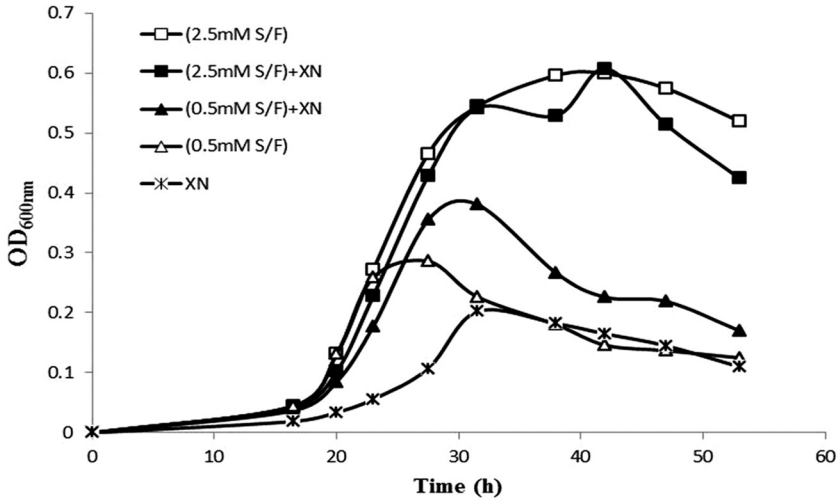

FIG 2 Growth of *Xcc*306 in sweetgum xylan with and without sucrose-fructose (S/F). Equal aliquots of an *Xcc*306 culture were inoculated into 6 culture tubes, (each) containing 4 ml of medium. All 6 cultures contained $XVM2_m$ with or without carbohydrates. □, 2.5 mM (each) sucrose and fructose; ■, 2.5 mM (each) sucrose and fructose and 0.25% sweetgum $MeGX_n$ (XN); ▲, 0.5 mM (each) sucrose and fructose and 0.25% sweetgum $MeGX_n$; ◇, 0.5 mM (each) sucrose and fructose; ∗, 0.25% sweetgum $MeGX_n$. Cultures were incubated at 28°C with shaking at 200 rpm.

y intercept, was used to calculate the number of molecules of RNA present in the sample.

RESULTS

Growth of *Xcc*306 in sweetgum xylan with and without sucrose-fructose. Bioinformatic studies of the sequenced genome of *Xcc*306 identified the presence of xylan utilization genes in *Xcc*306 and led us to investigate the growth characteristics of *Xcc*306 in sweetgum xylan. Purified methylglucuronoxylan ($MeGX_n$) from sweetgum wood was selected as a source of xylan, as it has been well defined in previous studies to be comprised almost exclusively of β-1,4-linked xylose residues variably modified with 4-*O*-methylglucuronate residues via α-1,2 linkages at a ratio of methylglucuronate to xylose of 1:6 to 1:7, with an estimated degree of polymerization of approximately 250 (3, 20). Acetyl groups were removed by KOH treatment during the preparation of $MeGX_n$. XVM2 medium was chosen because it was previously constituted for the investigation of *hrp* gene expression; however, in this study, the sucrose and fructose contents were reduced from 10 mM to 2.5 mM and 0.5 mM to discern growth attributed to xylan utilization. Figure 2 shows representative results from several experiments. When xylan polymer, $MeGX_n$, is the sole carbon source, *Xcc*306 grows poorly, attaining an OD_{600} of 0.20 at 31 h (Fig. 2). Several hours of lag time preceded exponential growth in xylan compared with the time to exponential growth in media which included sucrose and fructose. However, while the contribution to growth of $MeGX_n$ as the sole carbon source was not discernible in media with 2.5 mM sucrose and 2.5 mM fructose (Fig. 2, ■ and □ traces), an increase in growth of 0.1 OD_{600} unit (Fig. 2, an OD_{600} of 0.38 at 31 h [▲] minus an OD_{600} of 0.28 at 27 h [△]) was obtained in media with 0.5 mM sucrose and fructose.

Intracellular localization of xylanase activity. To find the cellular locations of these enzymes, cells were grown in media with and without xylan and tested for xylanase activity in the media and in crude cell fractions. The results are shown in Table 2. Media were concentrated to equal the volume of resuspended cell fractions, and these preparations were tested for xylanase activity in fluorescence-based assays monitored for 2 h. Xylanase activities between 0.12 and 0.17 U/mg were found exclusively in the cell fractions (Table 2) and not in any of the three concentrated culture media, in all of which the xylanase activities were less than 10^{-4} U/mg. Specific activity (U/mg) is defined as the number of micromoles of product per minute per milligram of protein for cytoplasmic preparations or purified cloned enzyme. By the fluorescent assay, cloned Xyn10A activity is 19.7 U/mg and Xyn10C activity is 1.3 U/mg. The specific activities of the purified cloned enzymes XynA2 from *Paenibacillus* sp. strain JDR2 and Xyn10A and Xyn10C from *Xcc*306 are also included in Table 2 for comparison.

To further investigate the subcellular localization of xylanase activities, *Xcc*306 cells were fractionated into periplasmic and cytoplasmic fractions. The results, shown in Fig. 3, indicate that the majority of activities are located in the periplasmic fractions. To verify the cell fractionation procedure, activities of a periplasmic enzyme, alkaline phosphatase (21), were also determined. Attempts to detect xylanase activities secreted by *Xcc*306 colonies grown on agar plates with xylan were not successful. Plates containing 0.5% oat spelt xylan in $XVM2_m$ overlaid with 500 μl of 50

TABLE 2 Xylanase activities in cell fractions and recombinant xylanases[a]

CF or rXyn	Medium composition or rXyn source(s)	Sp act[b]
CF 1	2.5 mM each S and F	0.126
CF 2	0.5 mM each S and F, 0.2% sweetgum xylan	0.174
CF 3	0.2% sweetgum xylan	0.150
Xyn10A	*Xcc*306	19.7
Xyn10C	*Xcc*306	1.3
XynA2	*Paenibacillus* sp. JDR2	21.6

[a] Cell cytoplasmic fractions (CF) were prepared from cultures of *Xcc*306 grown on $XVM2_m$ containing the indicated carbohydrate source(s) (S, sucrose; F, fructose). Pure recombinant xylanases (rXyn) were produced in *Escherichia coli* from the *xyn10A* and *xyn10C* genes from *Xcc*306 or the *xynA2* gene from *Paenibacillus* sp. JDR2.
[b] Specific activities are given as units (μmol product/min) per mg protein as determined by formation of the fluorescent product DiFMU.

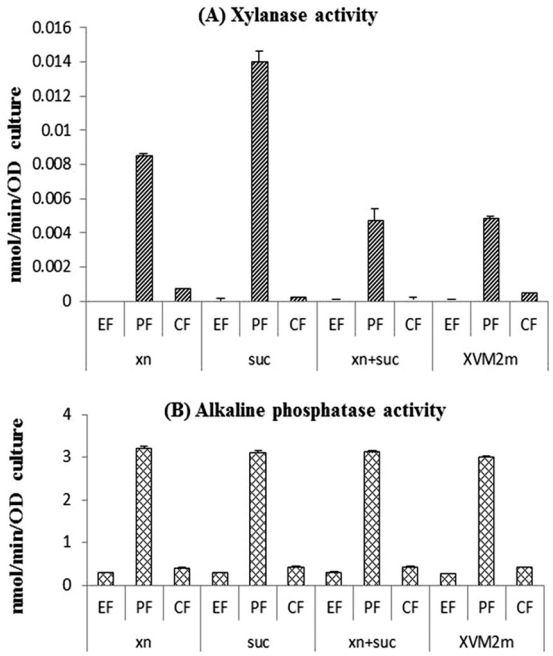

FIG 3 Xylanase activities in subcellular fractions. Xylanase activities were measured by the fluorescent assay using DiFMUX$_2$ as the substrate (A), and alkaline phosphatase activities were measured with *p*-nitrophenyl phosphate (B) as described in Materials and Methods. The culture media were 0.2% sweetgum xylan in XVM2$_m$ (xn), 2.5 mM sucrose in XVM2$_m$ (suc), 0.2% sweetgum xylan and 2.5 mM sucrose in XVM2$_m$ (xn+suc), and XVM2$_m$. The subculture fractions were the extracellular fraction (EF), periplasmic fraction (PF), and cytoplasmic fraction (CF). Since lysozyme was added to prepare the periplasmic fractions, enzymatic activity units are expressed as per OD_{600} of cell cultures instead of per protein concentration. Error bars represent error values from duplicate cultures.

mM each sucrose and fructose did not elicit, after 4 days, any halo formation surrounding these colonies as a measure of xylan hydrolysis and xylanase activities, in contrast to the distinct and plentiful halo formation by the control bacterium *Paenibacillus* sp. JDR2 (data not shown).

Growth promotion by oligoxylosides derived from xylan. To determine the role of GH10 xylanases and GH67 α-glucuronidase in *Xcc*306 growth, substrate utilization and growth characteristics were determined for both wild-type *Xcc*306 and the mutant strain of *Xcc*306 in which the α-glucuronidase gene is deleted (Fig. 4). XynA2 is a GH10 β-1,4 endoxylanase cloned from *Paenibacillus* sp. JDR2 that has been well defined with respect to activity and product formation (15). In media with xylan, both *Xcc*306 and *Xcc*306 Δ*agu67* showed moderate growth, to OD_{600}s of 0.15 and 0.11, respectively, utilizing the small amount of the oligoxylosides presumably generated by secreted xylanase (Fig. 4B and C). In media containing XynA2-hydrolyzed sweetgum xylan, *Xcc*306 and *Xcc*306 Δ*agu67* grew well, reaching OD_{600}s of 0.40 and 0.30, respectively (Fig. 4B and C), with further growth probably limited by the complete utilization of the oligoxylosides in the media. MeGX$_n$ (0.2%) supported exponential growth for 14 to 16 h, while XynA2-hydrolyzed MeGX$_n$ hydrolyzed by GH10 XynA2 sustained growth to 23 to 29 h. Each of the three major sources of oligoxylosides produced by hydrolysis of xylan, methylglucuronoxylotriose (MeGX$_3$), xylobiose (X$_2$), and xylose (X$_1$), was consumed over the 46 h of growth (Fig. 4B and C), while the majority of the nonhydrolyzed polymeric MeGX$_n$ initially present in the media was not utilized.

In media containing MeGX$_3$, *Xcc*306 consumed this tetrasaccharide and grew well, but *Xcc*306 Δ*agu67* did not utilize MeGX$_3$ for growth (Fig. 4A). When *Xcc*306 metabolized MeGX$_3$, neither xylotriose (X$_3$) nor X$_2$ was detected in the media (Fig. 4B), indicating that MeGX$_3$ was imported into the periplasm intact and hydrolyzed there or intracellularly. During growth of both the wild type and the Δ*agu67* mutant of *Xcc*306, free X$_1$ began to appear at late log phase of growth and was very slowly although completely consumed (Fig. 4B and C). Other experiments on the growth of *Xcc*306 in X$_1$ alone also showed much slower substrate consumption and cell growth than when it was grown in MeGX$_3$ (data not shown). *Xcc*306 Δ*agu67* containing a plasmid with the complete *agu67* gene restored the growth pattern for *Xcc*306 (Fig. 4A; unpublished data).

To determine whether Xyn10A or Xyn10C-hydrolyzed xylan would also support *Xcc*306 growth, sweetgum xylan was digested by purified Xyn10A or Xyn10C and added to XVM2$_m$. Either *Xcc*306 or *Xcc*306 Δ*agu67* was inoculated into these media. Both of these strains grew well, with similar growth characteristics in XynA2-hydrolyzed xylan, as shown in Fig. 4. All of the oligoxyloside products generated by either XynA2, Xyn10A, or Xyn10C hydrolysis were consumed by *Xcc*306, indicating that the assimilation and metabolism of the products of the xylanases were not rate-limiting steps (results not shown).

Coinduction and expression of xylan utilization genes. Real-time RT-PCR was performed to determine the influence on the expression of genes in the cassette illustrated in Fig. 1 by growth in MeGX$_n$ and oligoxylosides isolated from hydrolyzed MeGX$_n$. As shown in Fig. 5, expression of genes in the three opposing operons was induced by growth in sweetgum MeGX$_n$, oligoxylosides from Xyn10A-hydrolyzed MeGX$_n$, or oligoxylosides from Xyn10C-hydrolyzed MeGX$_n$ (Fig. 5A). Genes encoding glycoside hydrolase enzymes located in the upstream operon, *agu67* and *xyn43E*, and those located in the downstream operon, *xyn10A*, *xyn10B*, and *xyn10C*, were induced 1- to 4-fold when *Xcc*306 was grown in MeGX$_n$ and 24- to 366-fold when *Xcc*306 was grown in Xyn10A hydrolysates or Xyn10C hydrolysates (Fig. 5B). Gene *xyn43F*, encoding a β-xylosidase utilized in xylan depolymerization and positioned peripheral to these two operons, was induced 14- or 31-fold by a Xyn10A- or Xyn10C-derived hydrolysate, respectively, although there was a one-third reduction when the strain was grown in MeGX$_n$. Gene *cirA*, which encodes the TonB-dependent receptor, was induced 2-fold by MeGX$_n$ and 64- to 73-fold by the hydrolysates. Expression induction of the collection of genes probed within each operon decreases in the direction of transcription in the three operons that were analyzed, consistent with the effect of polarity in the transcription process (Fig. 5B). The genes *gyrB* and *atpD*, located outside the cassette and with functions unrelated to xylan utilization, are not induced (results not shown) by either xylan or its hydrolysates. The consensus of this and repeated experiments is that genes in this cassette are induced when *Xcc*306 is grown in media supplemented with xylan or oligoxylosides isolated from hydrolyzed xylan. The induction of expression is many times greater by oligoxylosides derived from xylan than by the xylan polymer; the extents of induction by oligoxylosides from Xyn10A hydrolysis and by Xyn10C hydrolysis of MeGX$_n$ are similar, and these responses are synchronous among the genes of the cassettes investigated.

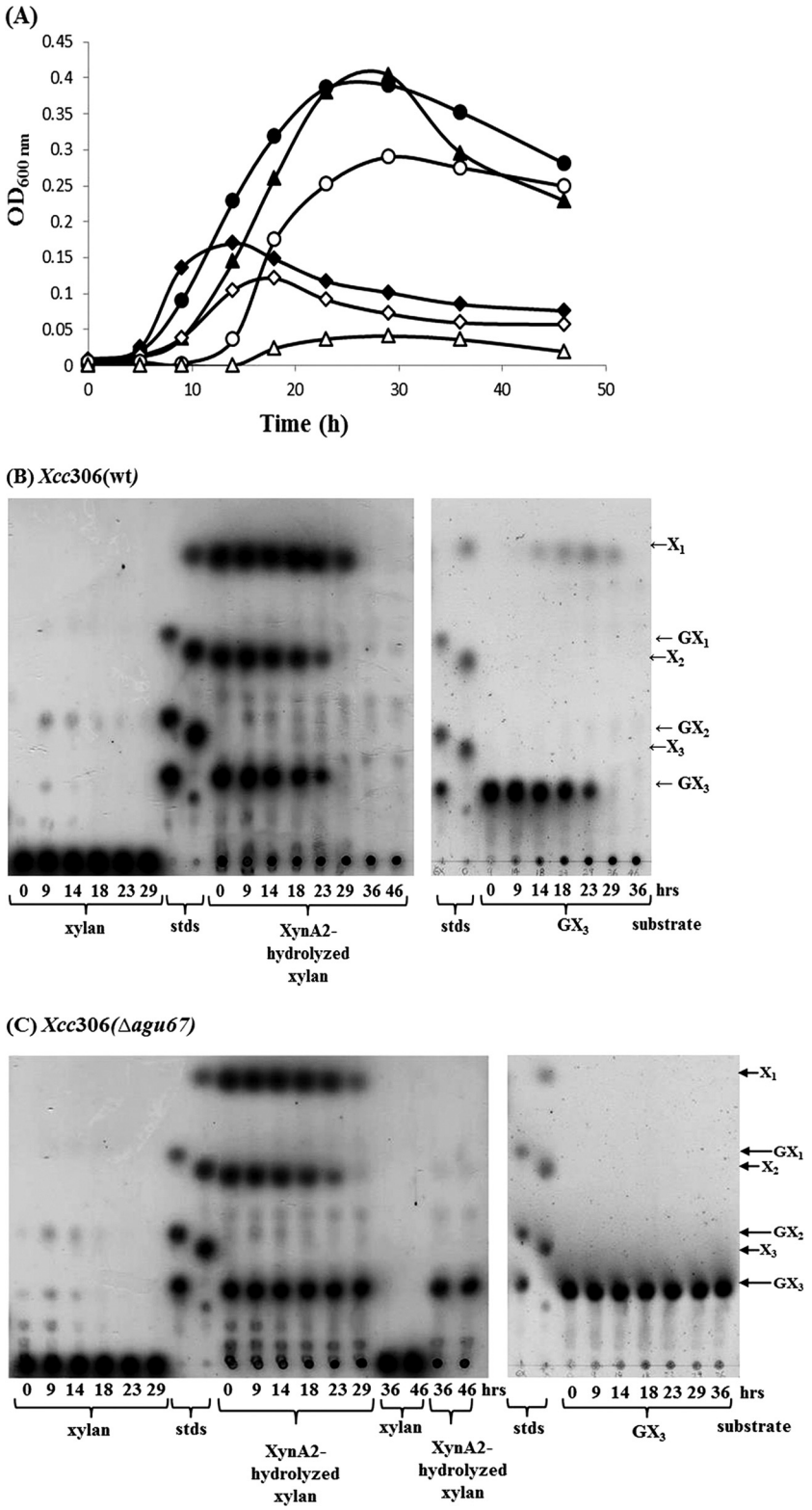

FIG 4 Growth of *Xcc*306 (wild type [*wt*]) and *Xcc*306 Δ*agu67* in XVM2$_m$ containing sweetgum MeGX$_n$ or depolymerized MeGX$_n$ products. (A) Two-milliliter samples of culture medium containing XVM2$_m$ and 0.2% sweetgum MeGX$_n$ (◆ and ◇), XynA2-hydrolyzed 0.2% sweetgum MeGX$_n$ (● and ○), or 0.2% (3.3 mM) MeGX$_3$ (▲ and △) were inoculated with an aliquot of either *Xcc*306 (◆, ●, ▲) or *Xcc*306Δ*agu67* (◇, ○, △) in nutrient broth at an OD$_{600}$ of 0.01. Cell cultures of Xcc306 (B) and Xcc306 Δ*agu67* (C) were incubated at 28°C with rotation at 200 rpm. Media taken at the times (in hours) after initiation of incubation were analyzed by thin-layer chromatography (TLC). Xylan, cultures with 0.2% sweetgum MeGX$_n$; stds, MeGX$_1$-MeGX$_3$ (10 nmol each) and X$_1$-X$_3$ (10 nmol each); XynA2-hydrolyzed xylan, cultures with 0.2% sweetgum xylan digested by XynA2; GX$_3$, cultures with 0.2% (3.3 mM) MeGX$_3$. Twelve microliters of the medium of each culture was spotted.

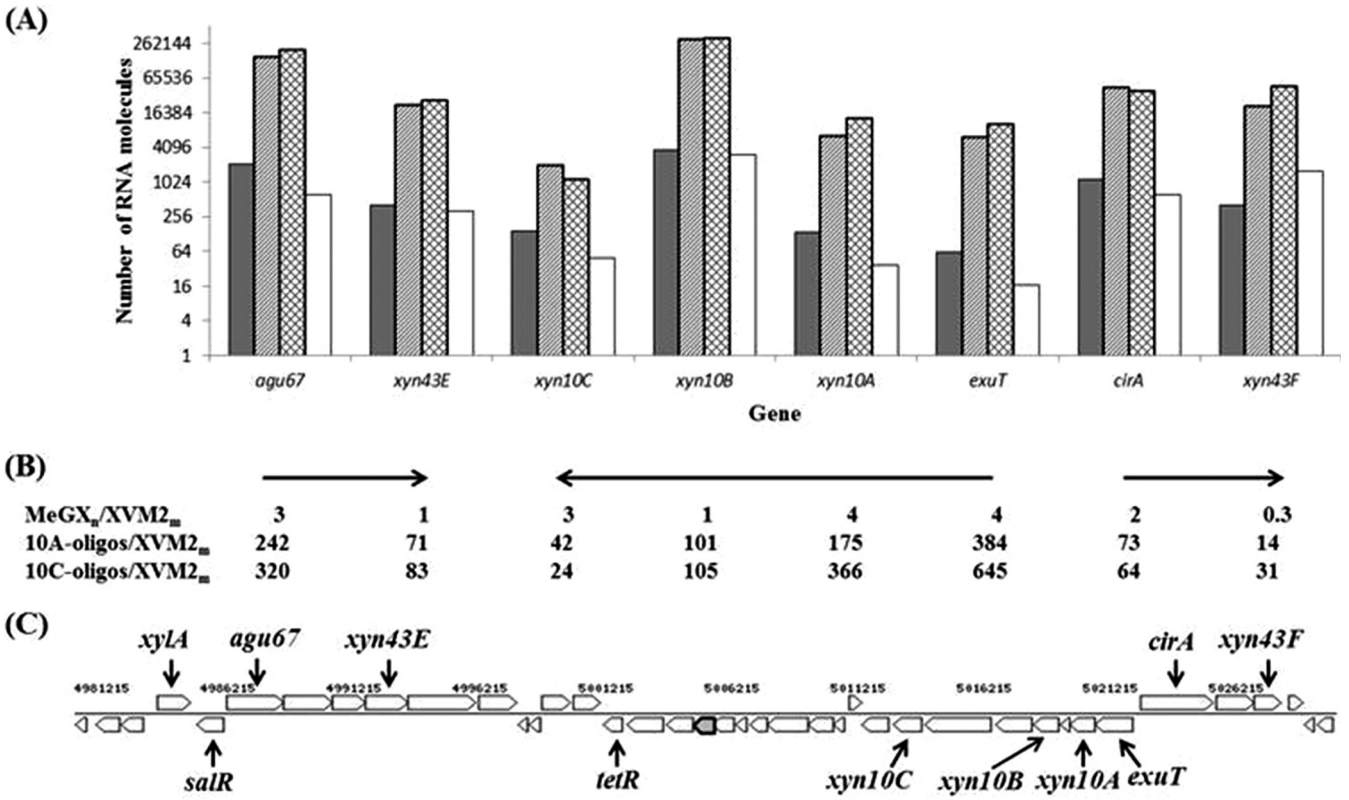

FIG 5 Expression of genes in the xylan utilization cassette of *Xcc*306. (A) Relative numbers of mRNA molecules expressed when *Xcc*306 is grown in MeGX$_n$ (dark-gray columns), in oligoxyloside mixtures of sweetgum MeGX$_n$ hydrolyzed by Xyn10A (light-gray columns), and by Xyn10C (hatched columns) and XVM2$_m$ (unfilled columns). (B) Ratios of mRNA molecules expressed by selected genes in *Xcc*306 cells grown in MeGX$_n$, in Xyn10A, and in Xyn10C oligoxylosides (oligos) relative to the ratio in *Xcc*306 cells grown in XVM2$_m$. Horizontal arrows depict transcriptional directions of gene clusters. (C) Diagram of the xylan utilization gene cassette in *Xcc*306.

DISCUSSION

A model for the depolymerization and uptake of xylan is presented (Fig. 6). When *Xcc*306 grows in the presence of xylan, it depolymerizes small amounts of xylan polymer to produce oligosaccharides for limited growth. Supplementing the amounts of oligoxylosides in the medium by supplying breakdown products of xylan by GH10 endoxylanases allows robust growth of *Xcc*306. MeGX$_3$, a breakdown product, is transported, possibly via the TonB-dependent receptor, to the periplasm, where the 4-*O*-methylglucuronyl group is released from the nonreducing terminal xylose by a membrane-bound GH67 α-glucuronidase enzyme located in the periplasm. Previous studies of *Cellvibrio japonicus* (*Pseudomonas cellulosa*) identified this enzyme to be associated with cellular membranes (22), and bacterial GH67 α-glucuronidases are commonly found as membrane-associated enzymes. In the periplasm, the released xylotriose products are processed by the endoxylanases Xyn10 to xylobiose. Conversion of xylotriose may also occur via the removal of the xylose residue from the nonreducing end by GH43 β-xylosidases, such as the protein product of the gene at locus XAC4183, as annotated by Integrated Microbial Genomes (IMG). Xylobiose and possibly xylotriose may be imported into the cytoplasm for further processing and metabolism. The transporter molecules involved in this trafficking have not been identified, and their hypothetical specificities and locations are included in the model.

We note that both xylanases Xyn10A and Xyn10C have a signal peptide which would translocate them to the periplasm during synthesis. However, we do not rule out the possibility that these enzymes are secreted to the extracellular space when *Xcc*306 grows on citrus tissues, perhaps in response to a plant signal (23). Two sources of the oligoxylosides for *Xcc*306 growth can be considered: one is xylan depolymerization by secreted *Xcc*306 xylanases, and the other is depolymerization by the host plant's xylanases.

In the first instance, we observe from our experimental results that *Xcc*306 xylanases are not found in significant levels in the medium (Fig. 3) and are therefore unavailable to depolymerize extracellular xylan. However, growth of *Xcc*306 *in planta* may provide secretion signals for these xylanases. This study shows induction of expression of genes encoding glycoside hydrolases, the transporter, and TonB-dependent receptor proteins by xylan and xylan hydrolysates. Dejean et al. (8) reported similar expression induction by xylo-oligosaccharide substrates in their investigation of the homologous genes in *X. campestris* pv. campestris. In the present study, when *Xcc*306 was grown in oligosaccharides derived from Xyn10A hydrolysate of xylan, increases in the expression of the *xyn10A*, *xyn10B*, *xyn10C*, and *agu67* genes relative to their expression in XVM2$_m$ media were 175-, 101-, 42-, and 242-fold, respectively, and the increase in the expression of the *cirA* gene was 73-fold (Fig. 5). When *X. campestris* pv. campestris was grown in xylotriose, the genes *xyn10A*, *xyn10C*, and *agu67* were induced 5-, 15-, and 25-fold, respectively, relative to their expression when the organism was grown in minimal media, while the

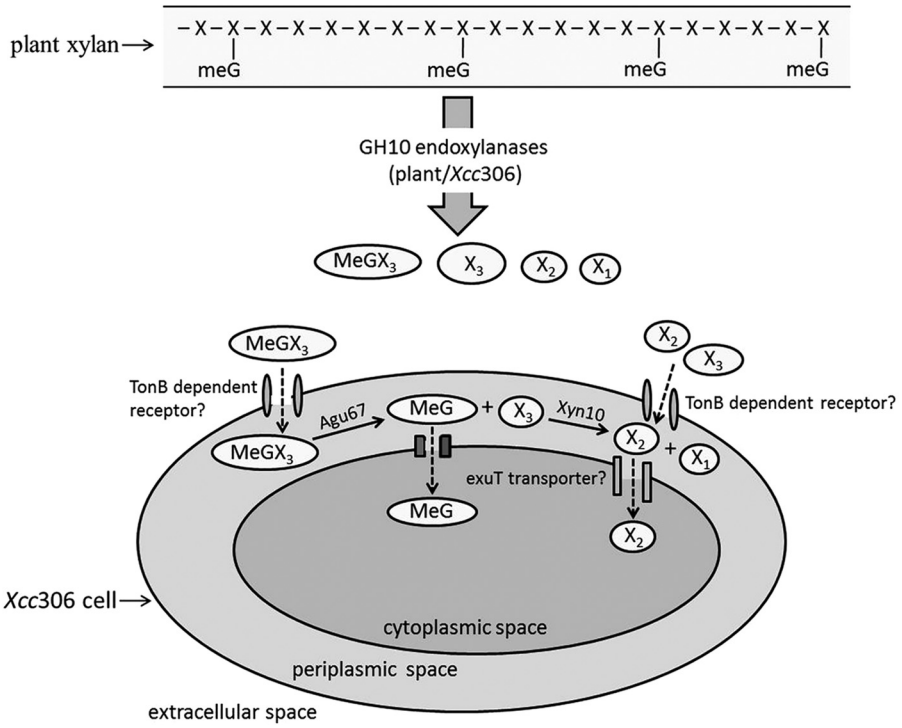

FIG 6 Model of xylan depolymerization and assimilation by *Xcc*306. The extracellular depolymerization of the methylglucuronoxylan ($MeGX_n$) generates predominantly $MeGX_3$, X_3, and X_2, as well as minor amounts of xylose, the ratios of which depend upon the frequency of the MeG substitutions. Oligoxylosides may be imported into the periplasm via TonB-dependent receptors and further processed within the confined periplasmic space prior to assimilation and metabolism.

TonB-dependent receptor-encoding gene *xytB* was induced 152-fold (8). However, the results of Dejean et al. (8) indicated an extracellular localization of endoxylanases, while the results of this study indicate their periplasmic localization in *Xcc*306.

The differing conclusions of xylanase localization may be partially due to the different culture conditions, the enzyme assays used to detect activity, the variable specific activities, and the repertoire of xylanase-encoding genes of the *Xanthomonas* species under study. Sun et al. (9) and Szczesny et al. (24) investigated the secretion of endoxylanases by the T2SS system and the role of endoxylanases in virulence in *Xanthomonas oryzae* pv. oryzae PXO99 and *Xanthomonas campestris* pv. vesicatoria 85-10, respectively. Sun et al. (9) described xylanase activity in both the extracellular and periplasmic spaces of *Xanthomonas oryzae* pv. oryzae. Szczesny et al. (24) found the *X. campestris* pv. vesicatoria Δ*xynC* mutant to induce less virulence in susceptible pepper plants. However, XynC (locus tag XCV0965) is an endoxylanase in the GH30 family and not in the GH10 family (XCV4355, XCV4358, and XCV4360) in *X. campestris* pv. vesicatoria. It should be noted that GH30 xylanases generate oligosaccharides that are not assimilated and metabolized without the assistance of another xylanase (1, 25, 26). *Xcc*306 differs from *X. campestris* pv. campestris, *Xanthomonas oryzae* pv. oryzae, and *X. campestris* pv. vesicatoria in that the corresponding gene in the *Xcc*306 genome that encodes the endoxylanase GH30 (previously designated GH5) is truncated (7) and therefore inactive. Since the *xyn10B* gene in Xcc306 does not encode a functional enzyme, xylanase activities expressed by *Xcc*306 are then solely due to the GH10 enzymes encoded by the genes *xyn10A* and *xyn10C* in the above-described cassette. The *xynB* gene may not encode a functional enzyme, as the NCBI-denoted translation start site results in a protein product without a secretion peptide and thus the xylanase synthesized would be an intracellular protein unable to act on xylan outside the cell or oligoxylosides located in the periplasmic space of the cell (unpublished). The recombinant forms of the Xyn10A and Xyn10C from *Xcc*306 have been shown to generate $MeGX_3$, X_3, and X_2 from $MeGX_n$ from citrus leaves and sweetgum wood (unpublished) and have recently been structurally defined (27). The coordinate expression of *xyn10* genes with the *agu67* gene ensures the assimilation of the maximal amount of oligoxylosides for complete metabolism of xylose derived from plant cell walls.

In considering the possible role of plant-derived endoxylanases in the depolymerization process, genes encoding GH10 endoxylanases are present in the *Citrus sinensis* genome (28; http://citrus.hzau.edu.cn/orange/index.php). A search for endoxylanase-encoding genes in *C. sinensis* yielded 5 such loci: Cs8g04100.1, Cs8g04110.1, Cs8g02850.1, Cs8g02860.1, and Cs3g16470.1. These putative endoxylanases belong to the GH10 family, and all contain the two requisite glutamate catalytic residues situated 107 to 109 amino acid residues apart (1). Transcriptome sequencing (RNA-seq) analysis (http://citrus.hzau.edu.cn/cgi-bin/orange/gene/Cs8g04110.1) showed that genes encoding four of these five endoxylanases (Cs8g02860.1 being the exception) are expressed abundantly in the leaves and fruit. Inspection of another recently sequenced X*anthomonas* host, *Solanum lycopersicum* (http://mips.helmholtz-muenchen.de/plant/tomato/searchjsp/index.jsp), also uncovered two genes that encode endoxylanases, also of the GH10 family. It had been noted that

young citrus trees are more susceptible to *Xcc*306 infection (29–31). It is possible that growth of young leaves involves the remodeling of xylan's structure (32) by the expression of the host plant's endoxylanases and that this results in a pool of oligoxylosides for uptake and growth of *Xcc*306.

Genes potentially encoding GH10 xylanases have been found in all of the sequenced genomes of plants, although there are no reports on the properties of plant GH10 xylanases. For GH10 endoxylanases from bacterial and fungal sources, the $MeGX_3$ generated from $MeGX_n$ and $MeGAX_n$ by a GH10 endoxylanase contains a methylglucuronate that is α-1,2 linked to the nonreducing terminal xylose, a requirement for processing by a GH67 α-glucuronidase to release xylotriose. The combination of the GH10 endoxylanases and the GH67 α-glucuronidases is necessary for the efficient depolymerization and catabolism of $MeGX_n$ and $MeGAX_n$ (1, 4, 15, 33). The presence of *xyn10* and *agu67* genes in *Xcc*306 and all other phytopathogenic xanthomonads supports a role for complete processing and metabolism of $MeGX_n$, including $MeGX_3$, as well as X_3 and X_2. There may be conditions under which photosynthates are limiting and an efficient xylan utilization system provides a survival advantage. It is noteworthy that this system is not common to other phytopathogenic bacteria. The absence of orthologs of *agu67* genes in any of the plant genomes supports a connection between cell wall reconstruction by plant GH10 enzymes and the availability of a preferred substrate for the proliferation of phytopathogenic xanthomonads.

A question arises when the robust growth of *Xcc*306 on oligoxylosides of depolymerized xylan is contrasted to *Xcc*306's minimal growth on xylan polymer. What might be the host plant's stimuli that initiate *Xcc*306 endoxylanase secretion or the pathogenic bacterial signals that promote plant endoxylanase production? Either of these events would result in the accumulation of oligoxyloside nutrients for *Xcc*306 and allow growth and colonization of the plant by the bacterial pathogen. Perhaps favorable conditions gained cumulatively in the microenvironment of the infected site may help *Xcc*306 establish an opportunistic and persistent infection in the citrus host. There is a noted absence in the sequenced genomes of any other phytopathogenic bacteria of genes encoding either a GH10 endoxylanase or a GH67 α-glucuronidase. The combination of these enzymes and the coregulation of their synthesis in all phytopathogenic xanthomonads suggest a unique role that contributes to their potential to cause plant disease.

ACKNOWLEDGMENTS

This research was supported by grant USDA-CSREES-SRGP-002216 and in part by Biomass Research & Development Initiative competitive grant 2011-10006-30358 from the USDA National Institute of Food and Agriculture.

REFERENCES

1. **Preston JF, Hurlbert JC, Rice JD, Ragunathan A, St John FJ.** 2003. Microbial strategies for the depolymerization of glucuronoxylan: leads to the biotechnological applications of endoxylanases. ACS Symp Ser **855:** 191–210. http://dx.doi.org/10.1021/bk-2003-0855.ch012.
2. **Kuhad RC, Singh A, Eriksson KE.** 1997. Microorganisms and enzymes involved in the degradation of plant fiber cell walls. Adv Biochem Eng Biotechnol **57:**45–125.
3. **St John FJ, Rice JD, Preston JF.** 2006. *Paenibacillus* sp. strain JDR-2 and XynA1: a novel system for methylglucuronoxylan utilization. Appl Environ Microbiol **72:**1496–1506. http://dx.doi.org/10.1128/AEM.72.2.1496-1506.2006.
4. **Chow V, Nong G, Preston JF.** 2007. Structure, function, and regulation of the aldouronate utilization gene cluster from *Paenibacillus* sp. strain JDR-2. J Bacteriol **189:**8863–8870. http://dx.doi.org/10.1128/JB.01141-07.
5. **Shulami S, Gat O, Sonenshein AL, Shoham Y.** 1999. The glucuronic acid utilization gene cluster from *Bacillus stearothermophilus* T-6. J Bacteriol **181:**3695–3704.
6. **Sawhney N, Preston JF.** 2014. GH51 arabinofuranosidase and its role in the methylglucuronoarabinoxylan utilization system in *Paenibacillus* sp. JDR-2. Appl Environ Microbiol **80:**6114–6125. http://dx.doi.org/10.1128/AEM.01684-14.
7. **Potnis N, Krasileva K, Chow V, Almeida NF, Patil PB, Ryan RP, Sharlach M, Behlau F, Dow JM, Momol M, White FF, Preston JF, Vinatzer BA, Koebnik R, Setubal JC, Norman DJ, Staskawicz BJ, Jones JB.** 2011. Comparative genomics reveals diversity among xanthomonads infecting tomato and pepper. BMC Genomics **12:**146. http://dx.doi.org/10.1186/1471-2164-12-146.
8. **Déjean G, Blanvillain-Baufumé S, Boulanger A, Darrasse A, Dugé de Bernonville T, Girard AL, Carrére S, Jamet S, Zischek C, Lautier M, Solé M, Büttner D, Jacques M-A, Lauber E, Arlat M.** 2013. The xylan utilization system of the plant pathogen *Xanthomonas campestris* pv. *campestris* controls epiphytic life and reveals common features with oligotrophic bacteria and animal gut symbionts. New Phytol **198:**899–915. http://dx.doi.org/10.1111/nph.12187.
9. **Sun Q, Hu J, Huang G, Ge C, Fang R, He C.** 2005. Type-II secretion pathway structural gene *xpsE*, xylanase- and cellulase secretion and virulence in *Xanthomonas oryzae* pv. *oryzae*. Plant Pathol **54:**15–21. http://dx.doi.org/10.1111/j.1365-3059.2004.01101.x.
10. **Gottig N, Garavaglia BS, Garofalo CG, Orellano EG, Ottado J.** 2009. A filamentous hemagglutinin-like protein of *Xanthomonas axonopodis* pv. *citri*, the phytopathogen responsible for citrus canker, is involved in bacterial virulence. PLoS One **4:**e4358. http://dx.doi.org/10.1371/journal.pone.0004358.
11. **Leite RP, Jr, Egel DS, Stall RE.** 1994. Genetic analysis of *hrp*-related DNA sequences of *Xanthomonas campestris* strains causing diseases of citrus. Appl Environ Microbiol **60:**1078–1086.
12. **Huguet E, Hahn K, Wengelnik K, Bonas U.** 1998. hpaA mutants of *Xanthomonas campestris* pv. *vesicatoria* are affected in pathogenicity but retain the ability to induce host-specific hypersensitive reaction. Mol Microbiol **29:**1379–1390. http://dx.doi.org/10.1046/j.1365-2958.1998.01019.x.
13. **Nelson N.** 1944. A photometric adaptation of the Somogyi method for the determination of glucose. J Biol Chem **153:**375–380.
14. **Ge Y, Antoulinakis EG, Gee KR, Johnson I.** 2007. An ultrasensitive, continuous assay for xylanase using the fluorogenic substrate 6,8-difluoro-4-methylumbelliferyl beta-D-xylobloside. Anal Biochem **362:** 63–68. http://dx.doi.org/10.1016/j.ab.2006.11.034.
15. **Nong G, Rice J, Chow V, Preston JF.** 2009. Aldouronate utilization in *Paenibacillus* sp. strain JDR-2: physiological and enzymatic evidence for coupling of extracellular depolymerization and intracellular metabolism. Appl Environ Microbiol **75:**4410–4418. http://dx.doi.org/10.1128/AEM.02354-08.
16. **Bessey OA, Lowry OH, Brock MJ.** 1946. A method for the rapid determination of alkaline phosphatase with five cubic millimeters of serum. J Biol Chem **164:**321–329.
17. **Hu N, Hung M, Chiou S, Tang F, Chiang D, Huang H, Wu C.** 1992. Cloning and characterization of a gene required for the secretion of extracellular enzymes across the outer-membrane by *Xanthomonas campestris* pv. campestris. J Bacteriol **174:**2679–2687.
18. **Rozen S, Skaletsky H.** 2000. Primer3 on the WWW for general users and for biologist programmers. Methods Mol Biol **132:**365–386.
19. **Bio-Rad Laboratories.** 2006. Real-time PCR applications guide. Bulletin 5279, p 2–6, 34–37. Bio-Rad Laboratories, Hercules, CA.
20. **Hurlbert J, Preston J.** 2001. Functional characterization of a novel xylanase from a corn strain of *Erwinia chrysanthemi*. J Bacteriol **183:**2093–2100. http://dx.doi.org/10.1128/JB.183.6.2093-2100.2001.
21. **MacAlister TJ, Costerton JW, Thompson L, Thompson J, Ingram JM.** 1972. Distribution of alkaline phosphatase within the periplasmic space of gram-negative bacteria. J Bacteriol **111:**827–832.
22. **Nagy T, Emami K, Fontes CM, Ferreira LM, Humphry DR, Gilbert HJ.** 2002. The membrane-bound alpha-glucuronidase from *Pseudomonas cellulosa* hydrolyzes 4-*O*-methyl-D-glucuronoxylooligosaccharides but not 4-*O*-methyl-D-glucuronoxylan. J Bacteriol **184:**4925–4929. http://dx.doi.org/10.1128/JB.184.17.4925-4929.2002.
23. **Wang Y, Kim SG, Wu J, Huh HH, Lee SJ, Rakwal R, Kumar Agrawal G,**

Park ZY, Young Kang K, Kim ST. 2013. Secretome analysis of the rice bacterium *Xanthomonas oryzae* (*Xoo*) using *in vitro* and in planta systems. Proteomics **13:**1901–1912. http://dx.doi.org/10.1002/pmic.201200454.

24. **Szczesny R, Jordan M, Schramm C, Schulz S, Cogez V, Bonas U, Büttner D.** 2010. Functional characterization of the Xcs and Xps type II secretion systems from the plant pathogenic bacterium *Xanthomonas campestris* pv *vesicatoria*. New Phytol **187:**983–1002. http://dx.doi.org/10.1111/j.1469-8137.2010.03312.x.
25. **St John FJ, Rice JJ, Preston JF.** 2006. Characterization of XynC from *Bacillus subtilis* subsp. *subtilis* strain 168 and analysis of its role in depolymerization of glucuronoxylan. J Bacteriol **188:**8617–8626. http://dx.doi.org/10.1128/JB.01283-06.
26. **Rhee MS, Wei L, Sawhney N, Rice JD, St John FJ, Hurlbert JC, Preston JF.** 2014. Engineering the xylan utilization system in *Bacillus subtilis* for production of acidic xylooligosaccharides. Appl Environ Microbiol **80:**917–927. http://dx.doi.org/10.1128/AEM.03246-13.
27. **Santos CR, Hoffmam ZB, de Matos Martins VP, Zanphorlin LM, de Paula Assis LH, Honorato RV, de Oliveira PSL, Ruller R, Murakami MT.** 2014. Molecular mechanisms associated with xylan degradation in *Xanthomonas* plant pathogens. J Biol Chem **289:**32186–32200. http://dx.doi.org/10.1074/jbc.M114.605105.
28. **Xu Q, Chen LL, Ruan X, Chen D, Zhu A, Chen C, Bertrand D, Jiao WB, Hao BH, Lyon MP, Chen J, Gao S, Xing F, Lan H, Chang JW, Ge X, Lei Y, Hu Q, Miao Y, Wang L, Xiao S, Biswas MK, Zeng W, Guo F, Cao H, Yang X, Xu XW, Cheng YJ, Xu J, Liu JH, Luo OJ, Tang Z, Guo WW, Kuang H, Zhang HY, Roose ML, Nagarajan N, Deng XX, Ruan Y.** 2013. The draft genome of sweet orange (*Citrus sinensis*). Nat Genet **45:**59–66. http://dx.doi.org/10.1038/ng.2472.
29. **Stall RE, Marco GM, de Echenique C.** 1982. Importance of mesophyll in mature-leaf resistance in cancrosis of citrus. Phytopathology **72:**1097–1100. http://dx.doi.org/10.1094/Phyto-72-1097.
30. **Brunings AM, Gabriel DW.** 2003. *Xanthomonas citri*: breaking the surface. Mol Plant Pathol **4:**141–157. http://dx.doi.org/10.1046/j.1364-3703.2003.00163.x.
31. **Gottwald TR, Graham JH, Schubert TS.** 12 August 2002. Citrus canker: the pathogen and its impact. Plant Health Prog http://dx.doi.org/10.1094/PHP-2002-0812-01-RV.
32. **Fry S.** 2004. Primary cell wall metabolism: tracking the careers of wall polymers in living plant cells. New Phytol **161:**641–675. http://dx.doi.org/10.1111/j.1469-8137.2004.00980.x.
33. **Biely P, Vrsanska M, Tenkanen M, Kluepfel D.** 1997. Endo-beta-1,4-xylanase families: differences in catalytic properties. J Biotechnol **57:**151–166. http://dx.doi.org/10.1016/S0168-1656(97)00096-5.